Modulation of Nucleotide Binding of *trans* Platinum(II) Complexes by Planar Ligands. A Combined Proton NMR and Molecular Mechanics Study

Ulrich Bierbach and Nicholas Farrell*

Department of Chemistry, Virginia Commonwealth University, Richmond, Virginia 23284-2006

Received February 12, 1997[⊗]

Nonclassical *trans* platinum complexes containing planar nitrogen bases show biological activity different from that of *trans*-diamminedichloroplatinum(II) (*trans*-DDP). In search of the mechanism of action of such compounds, a comparative study on the nucleobase chemistry of *trans*-DDP and *trans*-[$PtCl_2(NH_3)$(quinoline)] (*trans*-QUIN) was performed using 1D and 2D NMR spectroscopy and molecular modeling techniques. The two simple monofunctional adducts *trans*-[PtCl(9-ethylguanine-*N7*)(NH_3)L]NO_3 (L = NH_3, **1**; L = quinoline, **2**) were synthesized by employing the $AgNO_3$/DMF method. Reactions of these species with 5′-guanosine monophosphate (5′-GMP) and 5′-cytidine monophosphate (5′-CMP) were used to simulate potential second binding steps on DNA. Guanine-*N7* proved to be the kinetically preferred binding site for both **1** and **2**. Reactions with **2** proceeded significantly slower than those with **1** under the same conditions. These differences in reactivity are attributed to an altered hydrolytic behavior of **2** due to steric influences of quinoline upon associative substitution reactions. This is supported by interligand NOEs observed in the 2D NOESY spectrum of **2** and by AMBER-based geometries for different conformers of **2**. Signal splittings observed in the ^{1}H NMR spectra of **2** and the bifunctional adducts *trans*-[Pt(9-EtGua-*N7*)(5′-GMP-*N7*)(NH_3)L] (**4**) and *trans*-[Pt(9-EtGua-*N7*)$_2(NH_3)$L]$^{2+}$ (**6**) (L = quinoline) indicate hindered rotation about the Pt−N (guanine and quinoline) bonds. Temperature-dependent NMR spectra and molecular mechanics results are in agreement with frozen rotamers in solution at room temperature where unfavorable repulsive interligand interactions result in different head-to-head and head-to-tail orientations of the bases. For the different rotamers of **4**, a high barrier of interconversion of 87 kJ mol^{-1} was estimated from NMR data. The consequences of these kinetic and geometric effects with respect to target DNA are discussed.

Introduction

Numerous studies have focused on the binding of *cis*-[$PtCl_2(NH_3)_2$] (cisplatin, *cis*-DDP), a potent antitumor drug,[1] to potential biological target molecules. This area has been extensively reviewed.[2] An important question relating to the biological properties of cisplatin is why the corresponding *trans* isomer, *trans*-[$PtCl_2(NH_3)_2$] (transplatin, *trans*-DDP), has been found to be therapeutically inactive.[3] The structures of DNA adducts formed by the two isomers are distinctly different. Cisplatin preferably binds to N7 of two neighboring guanine bases (G) to form principally a 1,2 intrastrand (GG) cross-link[4] with lesser amounts of a similar 1,2 GA adduct. In contrast, *trans*-DDP lacks the geometrical requirements to produce this specific bifunctional adduct. Instead, alternative lesions, namely 1,3 intrastrand (GNG) cross-links[5] (Chart 1), are formed which tend to rearrange into bifunctional interstrand adducts.[6] Furthermore interstrand cross-links between N7 of guanine and N3 of cytosine of the same base pair (GC) have been detected *in vitro* (Chart 1).[7] This is in contrast to the situation for *cis*-DDP, where the interstrand cross-link is formed between guanines on adjacent base pairs.[8] Several theories have been put forward to explain the "geometrical discrimination" observed for the DDP isomers: (i) monofunctional adducts of *trans*-DDP with DNA (first binding step) are longer-lived than those of *cis*-DDP and may be quenched by intracellular thiols such as glutathione, preventing the formation of a toxic bifunctional lesion;[9] (ii) the impact of bifunctional DNA adducts on the globally modified DNA duplex is not as pronounced as that of the *cis* isomer and thus may affect replication to a lesser extent and/or lesions may be repaired more readily.[10] Characteristically, DNA damage recognition proteins containing the HMG

Chart 1

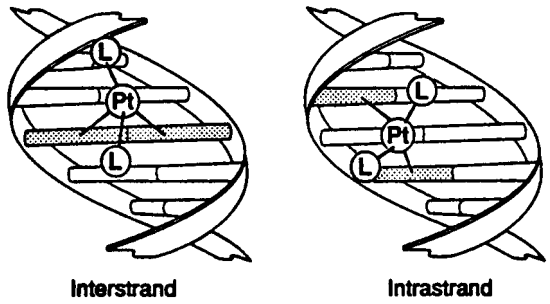

[⊗] Abstract published in *Advance ACS Abstracts,* July 15, 1997.

(1) Kelland, L. R.; Clarke, S. J.; McKeage, M. J. *Platinum Met. Rev.* **1992**, *36*, 178.
(2) (a) Reedijk, J. *Inorg. Chim. Acta* **1992**, *198*−*200*, 873. (b) Lepre, C. A.; Lippard, S. J. In *Nucleic Acids and Molecular Biology*; Eckstein, F., Lilley, D. M. J., Eds.; Springer: Berlin, 1990; Vol. 4, pp 9−38. (c) Sherman, S. E.; Lippard, S. J. *Chem. Rev.* **1987**, *87*, 1153.
(3) Farrell, N. In *Transition Metal Complexes as Drugs and Chemotherapeutic Agents*; Ugo, R., James, B. R., Eds.; Kluwer: Dordrecht, The Netherlands, 1989; Chapter 3 and literature cited therein.
(4) (a) Takahara, P. M.; Rosenzweig, A. C.; Frederick, C. A.; Lippard, S. J. *Nature* **1995**, *377*, 649. (b) Takahara, P. M.; Frederick, C. A.; Lippard, S. J. *J. Am. Chem. Soc.* **1996**, *118*, 12309.
(5) Farrell, N. *Met. Ions Biol. Syst.* **1996**, *32*, 603.
(6) Boudvillain, M.; Dallies, R.; Aussourd, C.; Leng, M. *Nucleic Acids Res.* **1995**, *23*, 2381.
(7) Brabec, V.; Leng, M. *Proc. Natl. Acad. Sci. U.S.A.* **1993**, *90*, 5345.
(8) (a) Hopkins, B. P.; Millard, J. T.; Woo, J.; Weidner, M. F.; Kirchner, J. J.; Sigurdsson, S. T.; Raucher, S. *Tetrahedron* **1991**, *47*, 2675. (b) Lemaire, M. A.; Schwartz, A.; Rahmouni, A. R.; Leng, M. *Proc. Natl. Acad. Sci. U.S.A.* **1991**, *88*, 1982.
(9) (a) Bancroft, D. P.; Lepre, C. A.; Lippard, S. J. *J. Am. Chem. Soc.* **1990**, *112*, 6860. (b) Eastman, A.; Barry, M. A. *Biochemistry* **1987**, *26*, 3303.

S0020-1669(97)00154-7 CCC: $14.00 © 1997 American Chemical Society

Chart 2

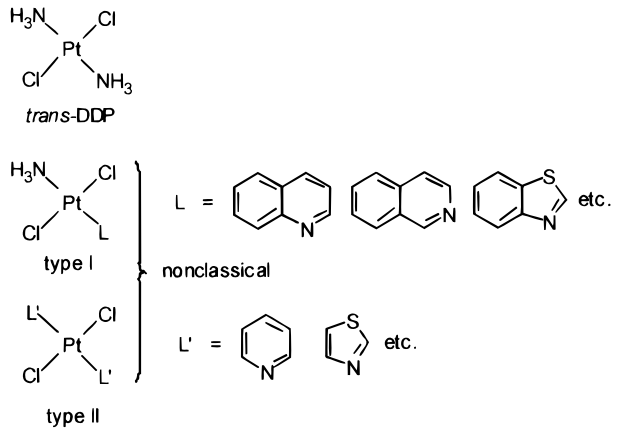

DNA binding motif bind to cisplatin-modified DNA but do not recognize *trans*-DDP-induced lesions.[11]

Two sets of *trans* platinum complexes have been identified which derive from *trans*-DDP by (partially) replacing the ammine ligands with planar N-containing heterocyclic bases (Chart 2).[5,12] The discovery of cytostatic activity for these compounds and the complexes *trans*-$[PtCl_2(HN{=}CRR')_2]$ (R = Me, R′ = OMe),[13] *t,t,t*-$[Pt^{IV}Cl_2(OH)_2$(cyclohexylamine)$(NH_3)]$, and *trans*-$[PtCl_2$(cyclohexylamine)$(NH_3)]$[14] added a new dimension to the discussion of the effects of *cis*−*trans* isomerism on the biological activity of platinum compounds. Compounds of types I and II (Chart 2) are of interest because they violate and, in some cases, even invert the classical structure−activity relationships for Pt-based antitumor compounds; i.e., it is possible that the *trans* isomer exhibits higher cytotoxicity than the *cis* isomer.[12] DNA-binding studies on *trans*-$[PtCl_2$(pyridine$)_2]$ indicate an alternative binding mode characterized by (i) an overall decreased rate of binding compared to that of DDP isomers, (ii) altered sequence specificity (GC) and DNA-unwinding properties, and (iii) a strong preference for *inter*strand cross-links.[5,15] These findings imply a modification of DNA that must be different from that caused by the drug *cis*-DDP.

In a systematic search for the mechanism of action of type I complexes we performed a comparative study on the nucleobase chemistry of *trans*-$[PtCl_2(NH_3)_2]$ (*trans*-DDP) and *trans*-$[PtCl_2$-(NH_3)(quinoline)] (*trans*-QUIN). We consider the latter quinoline-based compound a prototype of type I complexes, due to its biological activity and the availability of DNA-binding and protein recognition data.[5,16−18] In this paper we report the results of a model study on the formation and structure of the mono- and bifunctional *trans*-Pt−DNA adducts based on a proton NMR investigation and a molecular mechanics study employing the AMBER[19] force field. We chose the modified nucleobase 9-ethylguanine (9-EtGua) to simulate the first DNA-binding step and the simple mononucleotides 5′-guanosine monophosphate (5′-GMP) and 5′-cytidine monophosphate (5′-CMP) for the second step, i.e. DNA−DNA cross-link formation.

At this model nucleobase level, critical differences between *trans*-DDP and *trans*-QUIN emerge with respect to both the rate and the pathway of the second putative DNA-binding step as well as the final structures.

Experimental Section

Materials and Procedures. The starting complex *trans*-$[PtCl_2$-(NH_3)(quinoline)] was prepared by the published procedure[12] using freshly distilled quinoline. All other reagents and solvents were obtained commercially and used without further purification. The mononucleotides 5′-guanosine monophosphate and 5′-cytidine monophosphate were employed as their disodium salts (Aldrich). All procedures involving silver nitrate as reagent were performed in the dark.

Physical Measurements. ^{1}H NMR spectra were recorded at 300 MHz on a Varian Gemini-300 NMR instrument equipped with a variable-temperature unit and software for arrayed kinetic experiments. Except for nucleotide-binding studies and variable-temperature studies, spectra were obtained at 20 °C. Chemical shifts (δ, ppm) are referenced to TMS, except for spectra taken in D_2O, where DSS (4,4-dimethyl-4-silapentanesulfonic acid) served as internal standard. The 2D ^{1}H−^{1}H shift correlated spectrum (COSY) of **4** was acquired with a spectral window of 2830 Hz, 1024 data points, 256 t_1 increments (128 scans), and a relaxation delay time of 1 s between pulse cycles. The phase-sensitive 2D NOESY spectrum of **2** was acquired at 25 °C on a Varian Unity-Plus-500 instrument at 500 MHz with a spectral window of 7993 Hz, 2048 data points, 256 t_1 increments (64 scans), and a mixing time of 0.8 s. Proton-decoupled ^{195}Pt NMR spectra were taken at 64 MHz at 291 K with a solution of $K_2[PtCl_4]$ in D_2O as external standard. Shifts are reported vs $[PtCl_6]^{2-}$ standard (δ vs $Na_2[PtCl_6] = \delta$ vs $K_2[PtCl_4] - 1624$).

Chloride ion concentrations and pH values were determined at 21 °C with an Accumet 925 pH/mV meter equipped with a chloride-sensitive electrode (Fisher Scientific solid state ISE, Ag/AgCl reference electrode) and a Beckman combination electrode, respectively. All pH values taken of D_2O solutions are not corrected for the deuterium isotope effect and will be stated as pH* throughout the paper. Where necessary, pH values were adjusted with 0.1 M NaOD and DCl solutions. Elemental analyses were performed by Robertson Microlit Laboratories, Madison, NJ.

General Procedure for the Synthesis of *trans*-[PtCl(9-ethylguanine-*N7*)$(NH_3)_2$]NO_3 (1) and *trans*-[PtCl(9-ethylguanine-*N7*)(NH_3)(quinoline)]NO_3 (2). To a solution of 1 mmol of *trans*-$[PtCl_2(NH_3)_2]$ (*trans*-$[PtCl_2(NH_3)$(quinoline)] for **2**) in 25 mL of anhydrous DMF was added 0.170 g (1 mmol) of $AgNO_3$. After this mixture was stirred at room temperature for 16 h (48 h for **2**), precipitated AgCl was filtered off through a Celite pad. To the filtrate was added 0.179 g (1 mmol) of 9-ethylguanine, and the mixture was allowed to stir for 12 h (30 h for **2**). DMF was removed under reduced pressure at 30 °C. After addition of 50 mL of diethyl ether, the remaining oil solidified. Thus obtained crude products were recrystallized from methanol to give 0.380 g (white needles, yield 75%) of **1** and 0.410 g (light-yellow microcrystalline solid, yield 66%) of **2**, respectively. **1**: ^{1}H NMR (DMF-d_7) δ 1.44 (3 H, t), 4.16 (2 H, q), 4.31 (3 H, br), 7.24 (2 H, br), 8.60 (1 H, s), 11.50 (1 H, br); ^{195}Pt NMR (DMF-d_7) δ −2294. Anal. Calcd for $C_7H_{15}N_8ClO_4Pt$: C, 16.62; H, 2.99; N, 22.15; Cl, 7.00. Found: C, 16.61; H, 2.87; N, 21.91; Cl, 7.19. **2**: ^{1}H NMR (DMF-d_7) δ 1.27 (3 H, t), 4.00 (2 H, q), 4.70 (3 H, br), 7.21 (2 H, br), 7.73 (1 H, m), 7.77 (1 H, m), 7.97−8.01 (1 H, m), 8.14 (1 H, d, ^3J = 8.1 Hz), 8.67 (1 H, s), 8.70 (1 H, d, ^3J = 8.4 Hz), 9.61/9.62 (1 H, 2 d, ^3J = 5.4 Hz), 9.89 (1 H, d, ^3J = 8.4 Hz), 11.45 (1 H, br); ^{195}Pt NMR (DMF-d_7) δ −2198. Anal. Calcd for $C_{16}H_{19}N_8ClO_4Pt$: C, 31.10; H, 3.10; N, 18.13; Cl, 5.74. Found: C, 30.96; H, 3.13; N, 18.12; Cl, 5.52.

(10) Bruhn, S. L.; Toney, J. H.; Lippard, S. J. In *Progress in Inorganic Chemistry: Bioinorganic Chemistry*; Lippard, S. J., Ed.; Wiley: New York, 1990; pp 495−507.
(11) Pil, P. M.; Lippard, S. J. *Science* **1992**, *256*, 234.
(12) Van Beusichem, M.; Farrell, N. *Inorg. Chem.* **1992**, *31*, 634.
(13) Coluccia, M.; Nassi, A.; Loseto, F.; Boccarelli, A.; Mariggio, M. A.; Giordano, D.; Intini, F. P.; Caputo, P.; Natile G. *J. Med. Chem.* **1993**, *36*, 510.
(14) Mellish, K. J.; Barnard, C. F. J.; Murrer, B. A.; Kelland, L. R. *Int. J. Cancer* **1995**, *62*, 717.
(15) Zou, Y.; Van Houten, B.; Farrell, N. *Biochemistry* **1993**, *32*, 9632.
(16) Kharatishvili, M.; Mathieson, M.; Farrell, N. *Inorg. Chim. Acta* **1997**, *255*, 1.
(17) Marples, B.; Adomat, H.; Billings, P. C.; Farrell, N. P.; Koch, C. J.; Skov, K. A. *Anti- Cancer Drug Des.* **1994**, *9*, 389.
(18) Skov, K. A.; Adomat, H.; Doedee, M. J.; Farrell, N. *Anti-Cancer Drug Des.* **1994**, *9*, 103.
(19) Weiner, S. J.; Kollman, P. A.; Case, D. A.; Singh, U. C.; Ghio, C.; Alagona, G.; Profeta, S., Jr.; Weiner, P. *J. Am. Chem. Soc.* **1984**, *106*, 765.

Nucleotide-Binding Studies. The reactions between the monofunctional adducts (**1** and **2**) and the mononucleotides (5′-GMP, 5′-CMP) were performed at a concentration of 5 mM in both platinum and nucleobase in 99.96% D_2O at 37 °C in the NMR tube. All solutions were unbuffered (pH* 6.8−7.0). Alternatively, adducts **3**, **4**, and **6** were synthesized in deionized H_2O according to the above-mentioned conditions and lyophilized. ^{1}H NMR spectra were recorded at appropriate time intervals with 64 scans per time point. The first spectrum was acquired 12−15 min after mixing of the reactants, allowing the sample to adopt the nominal temperature and to eliminate temperature gradients. Arrayed spectra were recorded using the PAD command available in the Varian software. Quantitation of the progress of the reactions was achieved by integration of the nonexchangeable base protons H8 (5′-GMP, 9-EtGua), H5/H6 (5′-CMP), and H1′ of the ribose residue.

Molecular Mechanics Calculations. (a) Energy Minimization. Strain energies for the adducts **1**, **2**, **5**, and **6** were calculated with the all-atom AMBER force field[19] employing the module of HyperChem version 4.5 (1995).[20] Calculations were carried out either on a PC (120 MHz, 16 MB) or on an SGI workstation. Point minimizations employing the Polak-Ribiere minimizer were used to optimize the structures. A Δ rms gradient of 0.001 kcal/(mol Å^2) was chosen as the convergence criterion. For all calculations, the dielectric constant (ϵ) was set to the distance-dependent value of $4r_{ij}$. 1,4 electrostatic and van der Waals interactions were scaled by a factor of 0.5.

(b) Conformational Search. The systematic conformational search performed on **1**, **2**, **5**, and **6** was carried out with the appropriate module included in ChemPlus 1.0a (1994).[21] Calculations were based on a usage-directed scheme of the Monte Carlo multiple-minimum (MMCM) method.[22] For each planar base bound to platinum, one torsional angle that describes its dihedral angle with the platinum coordination plane (e.g., $H_3N-Pt-N7-C8$) was included in the random variations. The range of variation was 60−180°. Optimizations were carried out as described above. Only conformations with energies up to 5 kcal/mol above the lowest found were accepted and kept as potential new starting structures.

(c) Parametrization and Charge Distribution. Atom types and force field parameters were adopted from AMBER-type force fields which were recently developed by Hambley[23,24] and Marzilli[25] for modeling of adducts of the general type *cis*-[Pt(am)$_2$(G)$_2$] (am = NH_3, (am)$_2$ = diamine, G = guanine-containing DNA fragment). The guanine fragment was taken from the AMBER data base. One atom type for guanine-*N7* (NB) in **5** and **6** and one for the ammine ligands (N3) in **1** and **5** were introduced to unambiguously define the coaxial relationship of the ligands. All N−H distances provided by the AMBER data base were reduced by 10%. Parametrization of the free quinoline ligand was based on existing AMBER data (AMBER types CA and NC). Analogous force constants were used for platinated guanine and quinoline. The charge distribution for the guanine fragment was that provided by the AMBER data base. Fractional charges for quinoline were calculated with a combination of the Gasteiger−Marsili and Hückel methods included in the modeling package ChemPlus 1.0a/HyperChem 4.5. The assignment of fractional charges and the distribution of the 2+ charge on platinum onto the ligands followed a scheme introduced by Kozelka.[26] N1 of quinoline and N7 of 9-ethylguanine were treated in an analogous way. An estimated charge of −0.700 e was used for the chloro ligand. A list of force field parameters and charges is available as Supporting Information.

Results

Synthesis and Characterization of the Monofunctional Adducts. The preparation of *trans*-[PtCl(9-EtGua-*N7*)(NH_3)$_2$]-NO_3 (**1**) and *trans*-[PtCl(9-EtGua-*N7*)(NH_3)(quinoline)]NO_3 (**2**) followed a method described by Hollis (Scheme 1).[27] The reaction via monoactivated DMF species, *trans*-[PtCl(DMF-*O*)(am(m)ine)$_2$]$^+$, ensures the formation of the desired adducts. In contrast, direct treatment of *trans*-DDP with a nucleobase at a 1:1 ratio has been reported to give both mono- and (for our purposes undesired) disubstituted products, due to fast hydrolysis of the *trans*-Pt−Cl bond.[28] The use of 9-ethylguanine as the simplest conceivable "DNA model" proved to be advantageous for synthetic reasons. ^{1}H NMR data and their assignments for **1** and **2** are given in Table 1.

Scheme 1

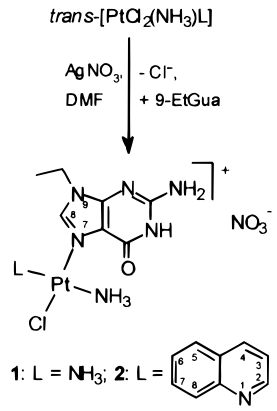

In both cases, ^{195}Pt NMR shifts[29] (see Experimental Section) and the pH dependence of δ for H8(9-EtGua)[30] are in agreement with an [N_3Cl] environment of Pt^{2+} and guanine coordination via N7.

The ^{1}H NMR spectrum of **2** in DMF-d_7 with an assignment of signals is shown in Figure 1. An expanded view of the H2 resonance of quinoline at δ 9.61 shows that the doublet with ^3J(H2,H3) $\approx$ 5 Hz splits into two signals of virtually equal integral intensity separated by only $\Delta\delta = 0.01$. However, all the other resonances, including that for H8 of guanine, show no splitting. This effect, which originates from restricted rotation within the Pt coordination sphere, proved to be a common spectroscopic feature for all the quinoline-containing adducts decribed in this paper and will be discussed in detail.

The 2D ^{1}H NOESY spectrum of **2** (Figure 2) shows cross-peaks due to strong NOEs for the atom pairs $H8_g/H8_q$ and $H8_g/H2_q$, which points to close interligand contacts between the *cis*-oriented quinoline (q) and guanine (g) bases. The rotamers for *cis*-oriented guanine and quinoline groups are head-to-head (HH) and head-to-tail (HT), similar to the situation discussed extensively for the solid state structures of *cis*-[Pt(9-EtGua)$_2$(NH_3)$_2$]$^{2+}$ salts.[31] Limited interconversion of these two forms produces either $H8_g\cdots H2_q$ or $H8_g\cdots H8_q$ close nonbonding distances (*vide*

(20) *HyperChem*, Release 4.5; Hypercube Inc.: Ontario, Canada, 1995.
(21) *ChemPlus, Extensions for HyperChem*, Release 1.0a; Hypercube Inc.: Ontario, Canada, 1994.
(22) Chang, G.; Guida, W. C.; Still, W. C. *J. Am. Chem. Soc.* **1989**, *111*, 4379.
(23) Hambley, T. W. *Inorg. Chem.* **1988**, *27*, 1073.
(24) Hambley, T. W. *Inorg. Chem.* **1991**, *30*, 937.
(25) Yao, S.; Plastaras, J. P.; Marzilli, L. G. *Inorg. Chem.* **1994**, *33*, 6061.
(26) Kozelka, J.; Archer, S.; Petsko, G. A.; Lippard, S. J. *Biopolymers* **1987**, *26*, 1245.
(27) Hollis, L. S.; Amundsen, A. R.; Stern, E. W. *J. Med. Chem.* **1989**, *32*, 128.
(28) Marcelis, A. T. M.; van Kralingen, C. G.; Reedijk, J. *J. Inorg. Biochem.* **1980**, *13*, 213.
(29) The ^{195}Pt resonances of **1** and **2** in DMF-d_7 appear ca. 100 ppm downfield of values that are usually observed for a mixed N_3Cl coordination of Pt^{2+} in aqueous solution. This solvent dependence of ^{195}Pt shifts has been reported before. See, for example: Ismail, I. M.; Sadler, P. J. In *Platinum, Gold and Other Metal Chemotherapeutic Agents*; ACS Symposium Series 209; American Chemical Society: Washington, DC, 1983; see also literature cited therein.
(30) Platinum coordination to N7 of guanine is the well-established binding mode under physiological conditions. Reaction conditions (aprotic solvent DMF, neutral pH) were chosen such as to only allow for N7 binding. Low-pH ^{1}H NMR spectra, not explicitly mentioned in this paper, consistently indicate no unplatinated N7 for all the adducts.
(31) Schöllhorn, H.; Raudaschl-Sieber, G.; Müller, G.; Thewalt, U.; Lippert, B. *J. Am. Chem. Soc.* **1985**, *107*, 5932.

Table 1. ^{1}H NMR Data for the Monofunctional Adducts **1** and **2**

	$\delta(^1H)$,[a] ppm												
		9-ethylguanine					quinoline						
compd, solv	NH_3	N1−H	H8	NH_2	$-CH_2-$	$-CH_3$	H8	H2	H4	H7	H5	H6	H3
1, DMF-d_7	4.31	11.50	8.60	7.24	4.16	1.44							
1, D_2O	n.o.[b]	n.o.	8.33[c]	n.o.	4.16	1.46							
2, DMF-d_7	4.70	11.45	8.67	7.21	4.00	1.27	9.89	9.61/9.62	8.70	7.97−8.01	8.14	7.77	7.73
2, D_2O	n.o.	n.o.	8.21[c]	n.o.	3.95	1.21	9.74	9.37/9.38	8.53	8.00−8.06[d]		7.76	7.58

[a] Assignments for **2** based on 2D NOESY spectra and selective spin-decoupling experiments (difference spectra); for multiplicity and coupling constants ^3J(H,H), see Experimental Section. [b] NH protons not observed due to rapid H,D exchange. [c] pH* 7. [d] Overlapping multiplets.

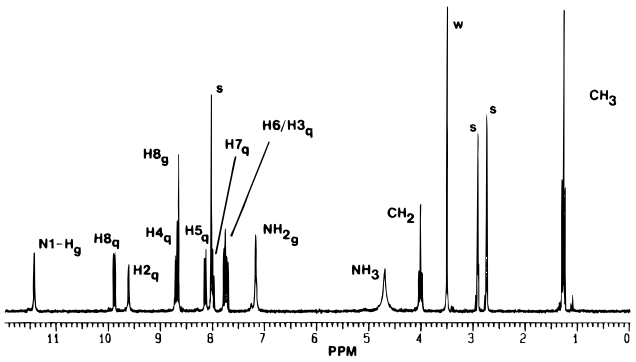

Figure 1. ^{1}H NMR spectrum of **2** (300 MHz, DMF-d_7) giving signal assignments. Indices g and q denote signals of the guanine and quinoline bases, respectively; s and w indicate residual solvent peaks and water (truncated).

infra). In addition, in DMF-d_7, where H,D exchange is slow, NOEs are observed between the aromatic protons $H8_g$, $H8_q$, and $H2_q$ and the ammine protons (Figure 2b). The order of intensity of the resulting cross-peaks was found to be $H8_g$/NH > $H8_q$/NH > $H2_q$/NH, which is in accordance with the *cis*/*trans* orientation of the ligands involved.

Kinetic Studies. Complexes **1** and **2** show a completely different behavior in aqueous solution. As determined by means of ion-sensitive measurements and ^{1}H NMR spectroscopy, aquation of **1** proceeds with a half-time of $t_{1/2} = 6-7$ h (at 37 °C, $c_{Pt} = 5$ mM), resulting in the release of free chloride. Under the same conditions, no hydrolysis is observed for **2**. Furthermore, attempts to abstract the chloro ligand with Ag^+ ions in water were successful for **1** (complete after 24 h) but failed for **2**, where no significant amount of precipitated AgCl was observed after 2 days.

The monofunctional adducts **1** and **2** were reacted with the mononucleotides 5′-GMP and 5′-CMP (Chart 3) under physiologically relevant conditions. The use of mononucleotides instead of the corresponding nucleobases proved to be advantageous for solubility reasons. In addition, it will be shown that the chiral ribose moiety can be exploited as an NMR probe (diastereomer formation) for hindered rotation within an asymmetric platinum coordination sphere. The aim was to study the affinity of both species **1** and **2** for a second nucleobase, i.e. the accessibility of the platinum center to a potential second DNA-binding step. The progress of the reactions was monitored by means of ^{1}H NMR specroscopy (depicted for the system **1** + 5′-GMP in Figure 3).

The presence of the quinoline ligand in **2** drastically slows the substitution of the second chloro ligand by both N7 of the G- and N3 of the C-base compared to analogous reactions with **1** (Figure 4; see also for reaction conditions and half-times). For both adducts, the reaction with 5′-GMP proceeds considerably faster than that with 5′-CMP. No significant accumulation of (aqua) intermediates was observed for the reactions of **1** and **2** with 5′-GMP. Substitution of chloride in **1** by N3 of 5′-CMP

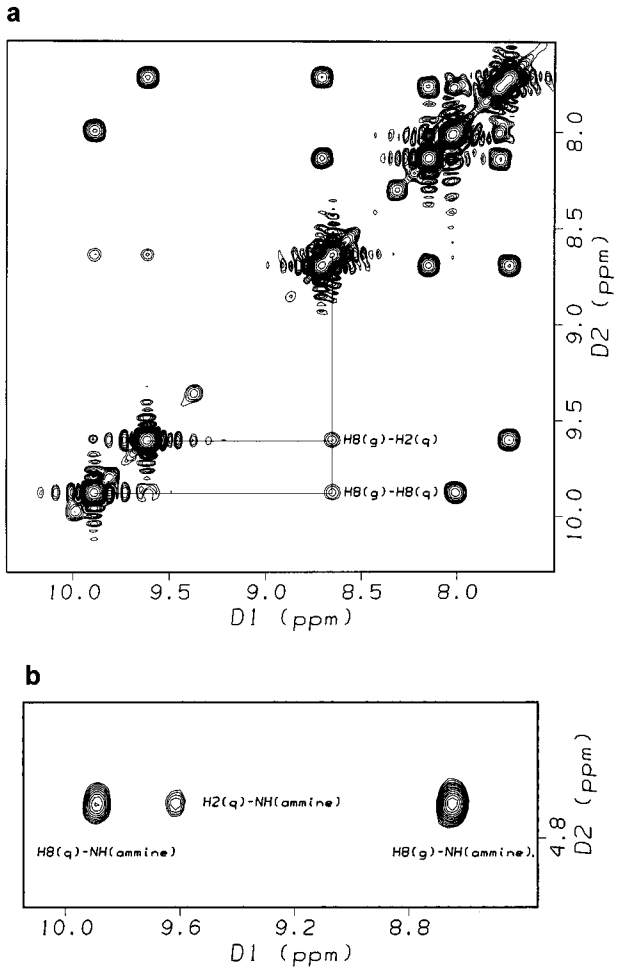

Figure 2. Selected regions of the 2D ^{1}H NOESY spectrum of **2** (500 MHz, DMF-d_7) showing cross-peak assignments: (a) aromatic region; (b) expanded section showing NOEs between the ammine ligand and *cis*- and *trans*-oriented bases.

proceeds very slowly, as evidenced by the appearance of two new doublets for H5 (δ 6.30) and H6 (δ 8.10) of the cytidine mononucleotide. As expected, both doublets appear slightly shifted to lower field compared to those of free 5′-CMP ($\Delta\delta_{H5} = 0.17$; $\Delta\delta_{H6} = 0.05$). However, the rate of hydrolysis of the Pt−Cl bond in **1** proved to be much faster ($t_{1/2} = 6.5$ h; see above) than the rate of Pt−base binding (Figure 4C). No substantial product formation was observed after incubating **2** with 5′-CMP for 48 h.

Structural Analysis of the Bifunctional Adducts. The 1:1 reactions between **1** and **2** and 5′-GMP gave the bifunctional adducts *trans*-[Pt(9-EtGua-*N7*)(5′-GMP-*N7*)(NH_3)$_2$] (**3**) and *trans*-[Pt(9-EtGua-*N7*)(5′-GMP-*N7*)(NH_3)(quinoline)] (**4**). No side products were detected. ^{1}H NMR data for **3** and **4** (Table 2) are in agreement with the *trans* adducts depicted in Chart 3. The assignment of base and sugar protons in **3** proved to be straightforward. The H8 resonances of 9-EtGua and 5′-GMP

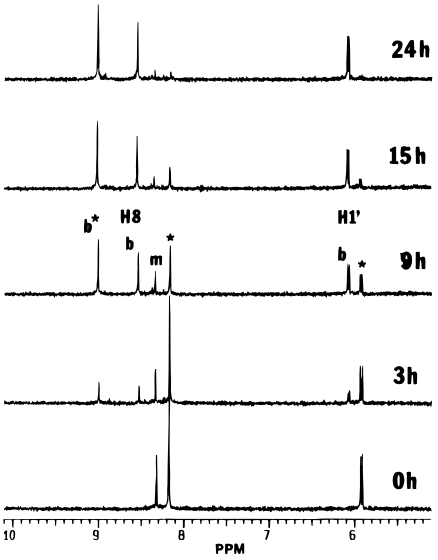

Figure 3. Progress of the reaction between **1** and 5′-GMP as monitored by ^{1}H NMR spectroscopy, showing characteristic changes in the H8/H1′ region. The asterisk denotes free 5′-GMP. Labels: m, monofunctional adduct (**1**); b, bifunctional adduct (**2**); b*, H8 of 5′-GMP in **2**.

Chart 3

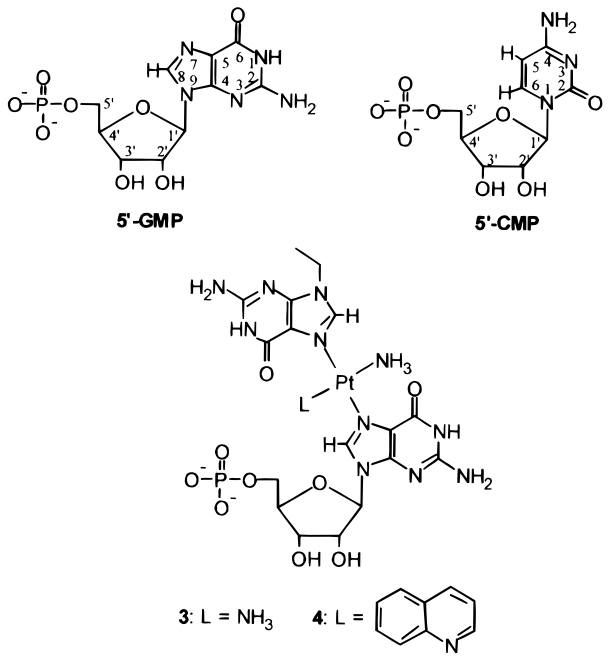

were assigned via pH dependence of the signals. Upon lowering of the pH* from 6.6 to 2.5, δ for H8(5′-GMP) experiences an upfield shift of 0.26 ppm due to protonation of the 5′-phosphate group.[32] In contrast, δ for H8(9-EtGua) is much less sensitive to changes in pH.

The assignment of signals for the quinoline-based adduct **4** was assisted by 2D ^{1}H−^{1}H shift correlated spectra (COSY). The ^{1}H NMR spectrum of **4** shows two doublets for $H2_q$ as already observed for **2** whereas H8 of 9-EtGua gives a sharp singlet (Figure 5). A 1:1 splitting of signals, however, is also observed for the base and sugar protons of the 5′-GMP ligand at both pH* 6.8 and 2.3. Formal replacement of 5′-GMP in **4** with 9-EtGua gives the species *trans*-[Pt(9-EtGua-*N7*)$_2$(NH$_3$)(quinoline)]$^{2+}$ (**6**). In this case, two $H2_q$ doublets but only one $H8_g$ singlet are found. Temperature-dependent ^{1}H NMR spectra

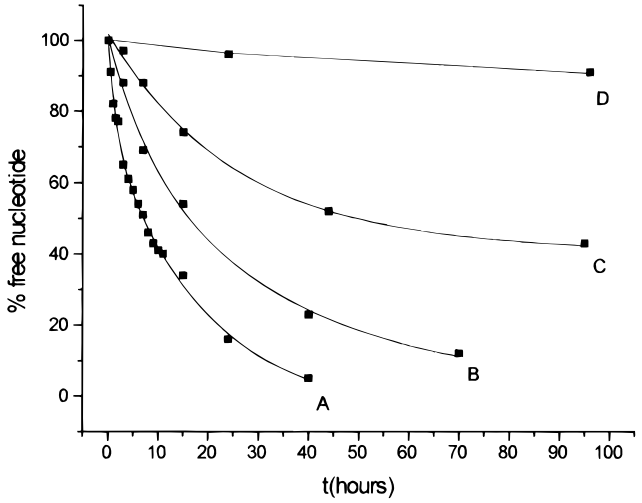

Figure 4. Kinetic profiles of the reactions of (A) **1** + 5′-GMP ($t_{1/2}$ = 7 h), (B) **2** + 5′-GMP ($t_{1/2}$ = 17 h), (C) **1** + 5′-CMP ($t_{1/2}$ = 50 h), and (D) **2** + 5′-CMP ($t_{1/2}$ not determined) in unbuffered D_2O solution. No significant change in pH* (maximum 0.2 pH* unit) was observed over the reaction periods. Conditions: $c_{Pt} = c_{nucl}$ = 5 mM, pH* 6.6−6.8, T = 310 K.

recorded for **4** show coalescence of signals above 70 °C as depicted for $H8_{g(5'\text{-GMP})}$ and $H2_q$ in Figure 6. This effect is accompanied by small but significant changes in chemical shifts, that appear most pronounced for $H8_g$ (upfield) and $H4_q$/$H5_q$ (downfield) upon going to higher temperatures (Figure 7).

Molecular Modeling. The principal strain-minimized conformers of the cations in **1**, **2**, **6**, and *trans*-[Pt(9-EtGua)$_2$(NH$_3$)$_2$]$^{2+}$ (**5**) as determined by a systematic conformational search are shown in Figures 8 and 9. Characteristic structural features and AMBER-minimized energies are given in Table 3. Symmetrically equivalent conformations found and those which only differ in the orientation of the ethyl group on the G-base were discarded.

For the cation of **1**, one conformation was found (Figure 8a). The energy-minimized structure is in excellent agreement with a recent X-ray structure[33] of the monofunctional *trans*-DDP−guanosine adduct (Supporting Information) despite solid state effects, such as hydrogen bonding involving nitrate counterions and crystal water. For all other cations, conformers were found as local minima with different head-to-head (HH) and head-to-tail (HT) orientations of the bases. The HH−HT terminology, which is similar to that applied to adducts of *cis*-DDP, is explained in the captions of Figures 8 and 9.

The *cis* orientation of quinoline and 9-ethylguanine in the cation of **2** gives rise to three conformers (Figure 8b) that are similar in energy. HH-1 proved to be the most favorable form and was found to be more stable than HT-0 and HT-1 by 3.32 and 4.39 kJ mol^{-1}, respectively. The increase in steric strain in the last two rotamers was found to be partly caused by repulsive interbase contacts between $H8_q$ and $H8_g$.

Four conformers were found for cation **5** (Figure 9a). The absolute value for the energy difference between the HH and HT conformations (i.e., the pairs HT-2/HH-2 and HH-1/HT-1) was as small as 0.53 kJ mol^{-1}. Analogous values for *cis*-[Pt(9-EtGua)$_2$(NH$_3$)$_2$]$^{2+}$ were found to be considerably higher in both Hambley's[23] and Marzilli's[25] calculations. This observation points to reduced interbase contacts in the coordination sphere of **5**, which consequently causes less steric strain for the *trans*-oriented guanine bases.

(32) Dijt, F. J.; Canters, G. W.; den Hartog, J. H. J.; Marcelis, A. T. M.; Reedijk, J. *J. Am. Chem. Soc.* **1984**, *106*, 3644.

(33) Arvanitis, G. M.; Gibson, D.; Emge, T. J.; Berman, H. M. *Acta Crystallogr., Sect. C* **1994**, *50*, 1217.

Table 2. ^{1}H NMR Data for the Bifunctional Adducts **3**, **4**, and **6**

	$\delta(^1H)$, ppm (^3J(H,H), Hz)[a]															
	9-ethylguanine			5′-GMP						quinoline						
	H8	$-CH_2-$	$-CH_3$	H8	H1′	H2′	H3′	H4′	H5′/H5″	H8	H2	H4	H7	H5	H6	H3
3	8.55[b] 8.50[d]	4.21	1.49	9.01[b] 8.75[d]	6.08 (4.9)	4.74	4.55	4.41	4.08[c]							
4	8.41[e] 8.73[g]	4.00	1.27	9.02/9.06[e] 8.39/8.40[g]	5.88/5.89 (5.4/5.3)	4.71/4.72	4.48/4.53	4.38	4.08[c]	9.80 (8.7)	9.60/9.57 (5.4/5.4)	8.41	8.00	7.80	7.56−7.66[f]	
6[h]	8.34	3.99	1.29							9.80 (8.9)	9.49/9.48 (5.3/5.4)	8.59	8.04−8.09[f]	7.78	7.63	

[a] All compounds 5 mM in D_2O; assignment of sugar and quinoline protons in **4** based on 2D COSY spectra. [b] pH* 6.6. [c] Center of ABM system. [d] pH* 2.5. [e] pH* 6.8. [f] Overlapping multiplets. [g] pH* 2.3. [h] pH* 7.0.

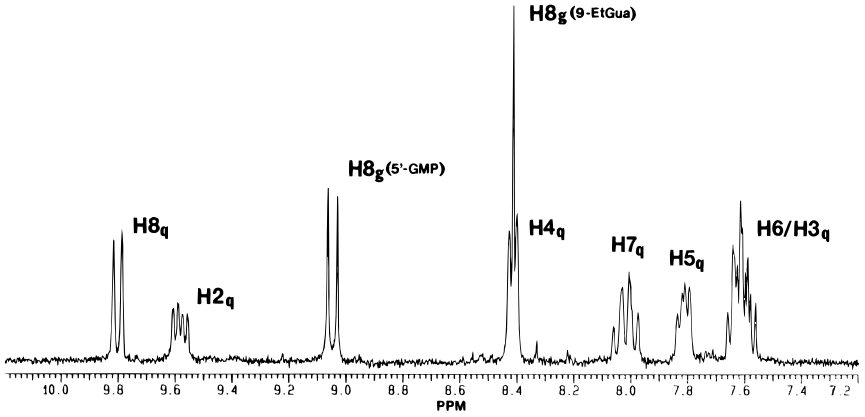

Figure 5. Aromatic region of the ^{1}H NMR spectrum of **4** (300 MHz, D_2O, pH* 6.6) giving signal assignments. Indices g and q denote signals of the guanine and quinoline bases, respectively. Note the 1:1 splitting of the resonances for $H2_q$ and $H8_{g(5'\text{-GMP})}$.

Three planar bases in the cation of **6** also result in four conformers characterized by different head-to-head and head-to-tail orientations of the quinoline and guanine bases (Figure 9b). Again, as observed for **2**, repulsive interactions between $H8_q$ and $H8_g$ (see Table 3) for conformers HTH-1 and HHT-0 cause unfavorable strain energies. The energy difference between conformers with an HH or HT orientation of the guanine bases was calculated to be smaller (0.97 kJ mol^{-1} between HHH-1 and HHT-1) than that for analogous rotamers of **5** (1.34 kJ mol^{-1} between HH-2 and HT-1). This effect, however, is mainly attributed to the presence of a second stabilizing hydrogen bond in **5**.

Discussion

Reactivity, Structure, and Molecular Dynamics. Different solvolysis behaviors have been established for *trans*-DDP and *trans*-QUIN (and other *trans* complexes containing planar bases). Displacement of the first chloro ligand by solvent molecules appears drastically slowed when a planar ligand is present.[5] This kinetic inertness also explains differences in chloride abstraction in DMF. *trans*-QUIN had to be reacted about 3 times longer with silver salt than *trans*-DDP to give a comparable quantity of precipitated AgCl. The same trend in reactivity prevails for the reactions between the nucleotides and the monofunctional adducts **1** and **2**, where, in turn, N7 of 5′-GMP proved to be the kinetically preferred binding site. This effect is in contrast to thermodynamic parameters that suggest comparable stability for the $Pt-N7_{5'\text{-GMP}}$ and $Pt-N3_{5'\text{-CMP}}$ bonds.[34] The rate of platinum binding to N3 may be affected by sterically unfavorable interactions caused by the exocyclic oxygen and NH_2 group in the 2- and 4-positions of the six-membered ring. In contrast, N7 of guanine appears to be much more accessible to platination. The kinetic preference for purine over pyrimidine binding was established previously for the *cis*-$[Pt(NH_3)_2]^{2+}$ fragment.[35]

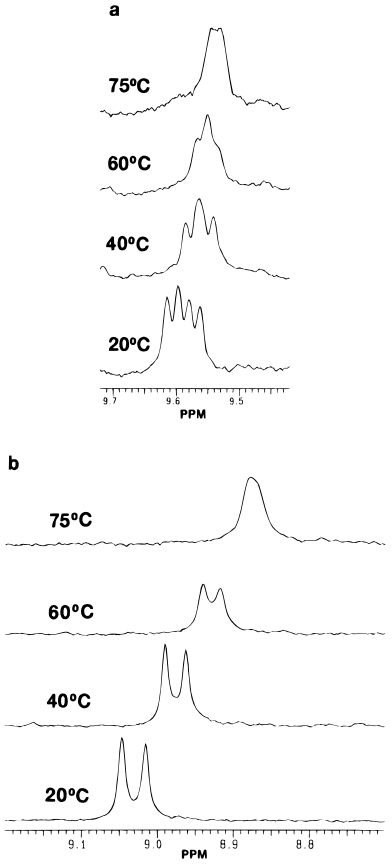

Figure 6. Variable-temperature ^{1}H NMR spectrum of **4** (300 MHz, 5 mM in D_2O): expanded views of (a) the $H2_q$ doublets and (b) the $H8_{g(5'\text{-GMP})}$ singlets.

(34) Scovell, W. M.; O'Connor, T. *J. Am. Chem. Soc.* **1977**, *99*, 120.

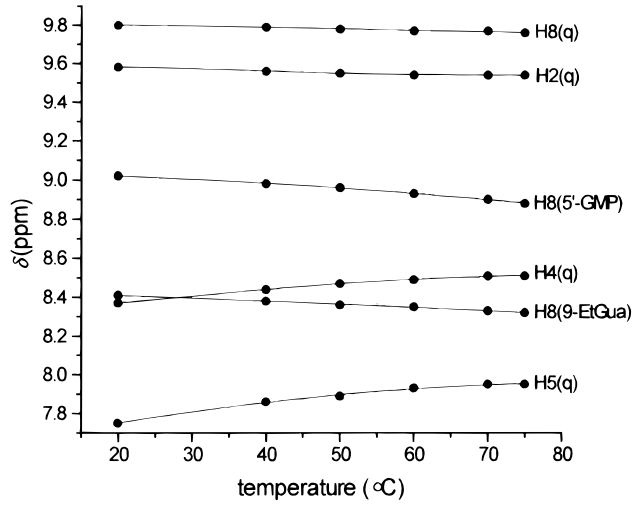

Figure 7. Plot of ^{1}H chemical shifts vs temperature of base protons in **4**.

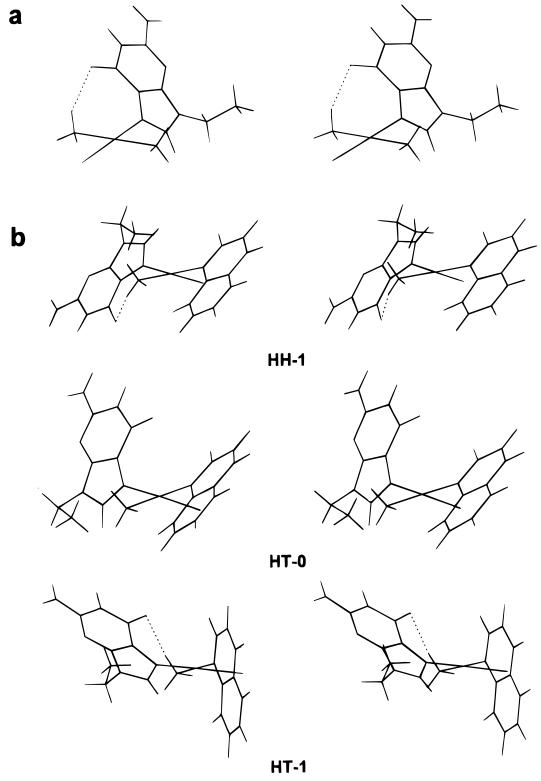

Figure 8. Stereoviews of energy-minimized conformations of **1** (a) and **2** (b). Energies increase from top to bottom. Intramolecular hydrogen bonds are indicated by dotted lines. For head-to-head and head-to-tail orientations, the five-membered ring of guanine and the six-membered N-containing ring of quinoline constitute the "heads" of the bases. An orientation with $H2_q$ and $H8_g$ located on the *same* side of the platinum coordination plane has been designated "HH" (head-to-head) and *vice versa*. The integer, separated by a hyphen, indicates the number of intramolecular hydrogen bonds found in each conformer.

Bifunctional adduct formation in reactions between **1** and 5′-GMP proceeds via the well-established two-step mechanism (for Pt(II) chloro ammine complexes) with reversible hydrolysis of the Pt−Cl bond that is thermodynamically favored at low chloride concentrations ($k_1 \gg k_3$ in Scheme 2).[32] This step then is followed by fast substitution of the aqua ligand by N7 of guanine. Characteristically, the rates of hydrolysis and nucleotide binding were determined to be identical ($t_{1/2} = 6-7$ h under conditions described earlier) for **1**. In contrast, lack of hydrolysis (less than 10% after 72 h) observed for **2** obviously favors a pathway involving direct substitution of the chloro ligand by strongly nucleophilic guanine-*N7* ($k_3 \gg k_1$). Displacement of any ligand other than the chloro ligand can be excluded after proper analysis of NMR data.

The kinetic studies reflect a pronounced influence of the

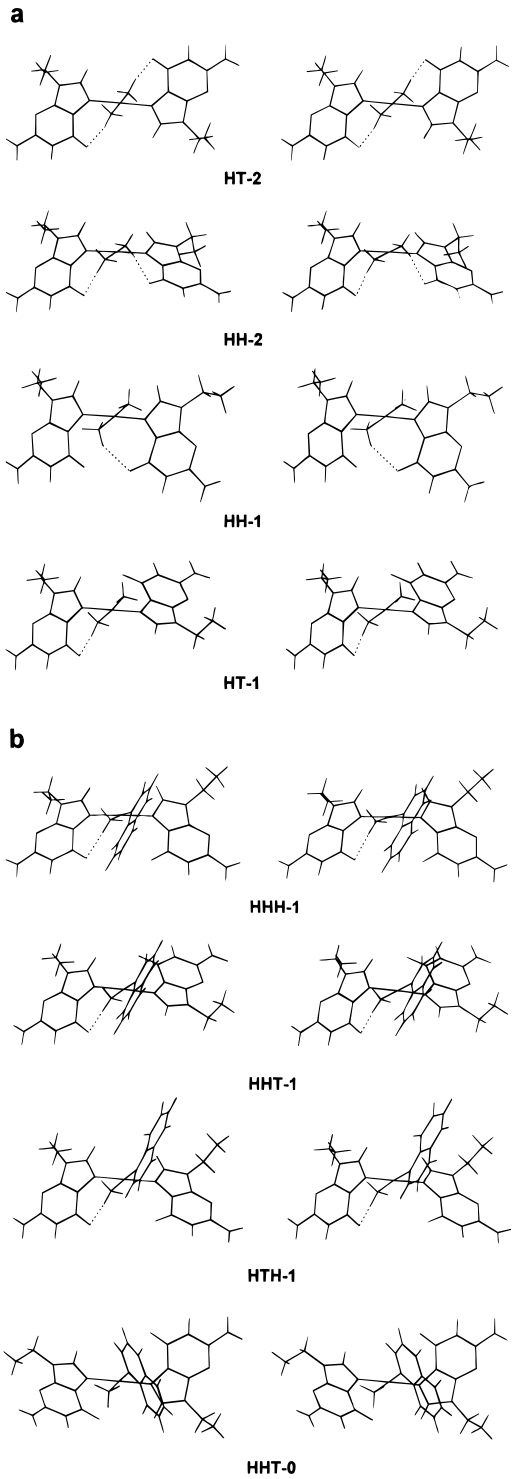

Figure 9. Stereoviews of energy-minimized conformations of **5** (a) and **6** (b). Energies increase from top to bottom. Intramolecular hydrogen bonds are indicated by dotted lines. For head-to-head and head-to-tail orientations, basically the same principles apply as introduced for **1** and **2**. HTH, for instance, means that the first guanine base and quinoline adopt a head-to-tail orientation (*HT*H) and the orientation of the guanine bases to each other is head-to-head (*HTH*).

(35) Mansy, S.; Chu, G. J. H.; Duncan, R. E.; Tobias, R. S. *J. Am. Chem. Soc.* **1978**, *100*, 607.

Table 3. Selected Structural Parameters and Energies for Strain-Minimized AMBER Geometries of **1**, **2**, **5**, and **6**

	G/Pt,[a] deg	G/G,[b] deg	HBD,[c] Å	H2(q)···H8(g), Å	H8(q)···H8(g), Å	E_{tot}, kJ mol^{-1}
1	53.4		2.95			−54.2
2						
HH-1	51.9	2.94	3.50	4.08	−23.6	
HT-0	62.2		5.72	2.63	−20.3	
HT-1	52.6	2.95	4.27	2.96	−19.3	
5						
HT-2 (C_i)		180.0	2.98			-69.3
HH-2 (C_2)		67.5	2.97			-68.7
HH-1		9.5	2.96 (3.25)[d]			-67.9
HT-1		123.5	2.97 (3.39)[d]			-67.4
6						
HHH-1		56.5	2.93	2.99/3.47	4.13/5.91	−61.2
HHT-1		117.5	2.96 (3.21)[d]	3.38/4.09	3.54/4.23	−60.2
HTH-1		54.5	2.93	3.97/5.59	2.56/3.42	−58.9
HHT-0		136.5		2.98/5.70	2.59/5.90	−57.5

[a] Angle between Pt coordination plane and guanine bases. [b] Angle between guanine bases. [c] *d*(O6···N(ammine)). [d] O6 atoms of both guanine bases interact with the ammine ligand in an asymmetric way, giving one "normal" H-bond and one weaker attraction.

Scheme 2

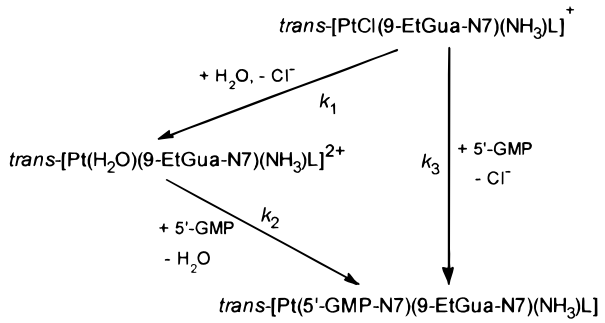

quinoline base on associative substitution reactions on the Pt^{2+} center. The 2D NOESY spectrum of **2** showed cross-peaks that reveal interligand (*trans*!) NOEs between the ammine protons and $H2_q$ and $H8_q$ of quinoline. These findings support an orientation of the quinoline ligand that must be considered perpendicular to rather than coplanar with the Pt coordination plane. This is in accordance with the AMBER-based models of **2**, where the angle between the planes through quinoline and the platinum coordination sphere adopts values of ∼60° (HH-1, HT-0) and ∼82° (HT-1), respectively. NOE intensities can be related to intramolecular nonbonding distances found in energy-minimized conformations of **2**. Two strong cross-peaks of virtually equal intensity are observed for the contacts $H2_q$···$H8_g$ (3.5 Å in HH-1) and $H8_q$···$H8_g$ (3.0 Å in HT-1), which supports a 1:1 population of the different rotamers in solution. The observed geometries that minimize interbase contacts, however, should be unfavorable for an axial nucleophilic attack on platinum, which would explain the kinetic inertness of **2**.

The splitting of the $H2_q$ signal in ^{1}H NMR spectra of **2**, **4**, and **6** proved to be the most striking spectroscopic feature of all the quinoline-containing adducts. Both homo- and heteronuclear couplings and *cis*−*trans* isomerizations in these systems can be excluded as the source for this effect. Intermolecular base stacking in solution can also be ruled out, since no concentration dependence is observed for the signal splittings. Consequently, restricted interconversion on the NMR time scale of different rotamers of these species remains as the only plausible explanation. The low rate of intramolecular rotation has to be attributed to repulsive interactions between the *cis*-oriented guanine and quinoline bases. Slow rotation about the Pt−N7 and Pt−N1 bonds then leads to the following situation: the quinoline ligand experiences two basically different environments. For the monofunctional adduct **2**, a head-to-head and a head-to-tail orientation of the planar bases is possible. In **4** and **6**, quinoline "sees" either a head-to-head (HHH, HTH) or a head-to-tail (HHT) orientation of the slowly rotating guanine bases. According to integral intensity ratios of the $H2_q$ NMR signals, HH and HT rotamers must be equally populated. In these rotamers $H2_q$ experiences a slightly different environment whereas chemical shifts of all the other signals, including those of $H8_g$ and the methyl(ene) protons of 9-ethylguanine in **2** and **6**, are not affected to the same degree and coincidentally coalesce.

An interesting spectroscopic feature proved to be the 1:1 splitting of ^{1}H NMR signals of 5′-GMP in **4**. Two sets of signals are also detected at low pH. Thus the splitting of the 5′-GMP resonances is not likely to result from dynamic effects caused by intramolecular hydrogen bonds of the type O_3PO···HN. The NMR results can be reliably explained when one considers the unsymmetric environment of platinum in **4** (unlike that in **6**) and the chirality of the (*R*)-ribose residue of the nucleotide. Hindered rotation about the Pt−N bonds will produce pairs of diastereomers for each frozen rotamer, causing inequivalence of those protons that are close to the center of chirality: in a frozen isomer such as HHH-1 of **6** (Figure 9b), for instance, formal alternative replacement of one 9-EtGua with 5′-GMP gives two spectroscopically distinguishable species.

The shape and separation of the two $H2_q$ doublets in the ^{1}H NMR spectrum of **4** allowed for an estimation of the barrier of isomer interconversion. With a first-order rate constant of $k_c = 24$ s^{-1} (based on the $H2_q$ line separation, $\Delta\nu = 11$ Hz) and a coalescence temperature of $T_c = 343$ K, a free energy of activation of $\Delta G^{\ddagger} \approx 87$ kJ mol^{-1} was calculated. This proves to be an exceptionally high barrier, and comparable values have only been reported for *cis*-bis(guanine) adducts of platinum with sterically demanding nonleaving groups.[36]

The upfield shifts observed for proton resonances both of H8 in the guanine bases and of $H2_q$ and $H8_q$ (Figure 7) in **6** with increasing temperature reflect altered ring-current effects due to dynamic processes. A similar effect has been reported for *cis*- and *trans*-[Pt(5′-GMP)$_2$(NH$_3$)$_2$].[28] Enhanced rotation about the Pt−N bonds should favor conformations where these protons are located above the plane of a neighboring aromatic ligand. An opposite temperature dependence is observed for $H4_q$ and $H5_q$. This downfield shift may also be related to the relative orientation of the quinoline and the guanine bases.

A comparison of strain-minimized conformations of *trans*-[Pt(9-EtGua-*N7*)$_2$(NH$_3$)$_2$]$^{2+}$ (**5**) with those found for *trans*-[Pt-(9-EtGua-*N7*)$_2$(NH$_3$)(quinoline)]$^{2+}$ (**6**) shows that quinoline

(36) Cramer, R. E.; Dahlstrom, P. L. *J. Am. Chem. Soc.* **1979**, *101*, 3679.

restricts the orientation of the guanine bases. In all conformations of **6**, the planar ligands are arranged in a conrotatory propeller-like way such as to minimize interligand repulsion. Furthermore, quinoline reduces the number of possible orientations of the guanine bases *trans*-oriented to each other: angles between the guanine planes of 180.0 and 9.5° found in **5** for the conformers HT-2 and HH-1 (Figure 9a), respectively, are not observed for **6**. In addition, head-to-head and head-to-tail conformers of both adducts with analogous structures (e.g., HH-2 of **5** and HHH-1/HTH-1 of **6**) significantly differ in GG interbase angles. As can be seen from the data presented in Table 3, quinoline also alters the relative order of conformer stabilities. The HHH-1 form represents the global minimum for **6** whereas the HT-2 form was found to be the lowest-energy conformation of **5**. This order, however, determined in an isolated environment, also depends on the number of hydrogen bonds present and does not necessarily reflect the situation in aqueous solution and in the solid state, where *inter*molecular H-bonds may dominate. The same applies to HH-1 and HT-0 of **2**, where the energy difference is supposed to be smaller in aqueous solution, which would in fact support the observed 1:1 population of the different conformers.

Possible Biological Consequences. Brabec and Leng showed, at least for *trans*-DDP, that GC predominates over GG interstrand adduct formation under competitive conditions.[7] Our model study clearly shows that this binding mode does not reflect the kinetic preference for the bases but may be enforced by steric factors present in duplex DNA. In the presence of a sterically demanding planar nonleaving group, a GG cross-link, rather than GC, appears favorable for steric reasons. However, both the low rate of formation of the bis(guanine) adduct **4** and the observed restricted rotation about the Pt−N bonds in the mono- and bifunctional adducts (**2**, **4**, and **6**) may make the GG cross-link unfavorable when competitive biological targets (e.g., donor atoms of proteins) are present. High barriers of rotamer interconversion indicate reduced steric flexibility. This could be of importance both for the conversion of a mono- into a bifunctional adduct on DNA and for the steric strain produced by such a cross-link.

The tendency of the quinoline-based compound to effectively form long-lived monofunctional adducts on DNA, due to lack of hydrolysis and steric factors, clearly differentiates the nonclassical *trans* platinum geometry from that of *trans*-DDP and suggests possible effects on DNA binding.

First, the hydrolytic behavior of a monofunctional DNA adduct could favor the binding of sulfur-containing protein side chains. Methionine and cysteine sulfur binding to platinum drugs is known to proceed rapidly, and without prior aquation of the Pt−Cl bond.[37] Introduction of a planar ligand such as quinoline may effectively modulate the ratio of nitrogen (DNA) to sulfur (protein) binding (second step) and the stability of a *trans*-*S*−Pt−N7 adduct. Platinum-mediated DNA−protein cross-linking was recently demonstrated for a *cis*-dichloroplatinum(II) complex that carries a bulky bicycloheptane-substituted diamine nonleaving group. Monofunctional adducts on DNA formed by this species convert into bifunctional adducts ($t_{1/2}$ > 8 h) with a lower rate than analogous adducts of *cis*-DDP ($t_{1/2}$ < 3 h) and are able to efficiently trap *Escherichia coli* DNA repair (endonuclease) proteins.[38] In this respect, it is noteworthy that protein-associated DNA strand breaks have been found as a consequence of cellular DNA damage induced by our new *trans* platinum complexes.[5] The exact identity of the protein is still under investigation. DNA−protein cross-links are assumed to be the major lesion induced by topoisomerase poisons.[39] An irreversible trapping of topo I or II or other DNA-processing proteins appears to be an attractive mode of action.[40,41]

Second, a combination of monofunctional N7 binding and stacking interactions of the planar ligand with adjacent nucleobases of the DNA strand may be an initial step in the mode of action. The cationic complex *cis*-$[PtCl(chloroquine)(NH_3)_2]^+$ is stereochemically compatible with both an intercalating mode and covalent binding.[42] Upon monofunctional binding to DNA, the chloroquine complex would produce a situation analogous to **2**, with mutually *cis*-oriented guanine and a quinoline-based intercalator. The combined ("pseudobifunctional") covalent binding/intercalation mode could have consequences for DNA conformation changes and protein recognition.[43]

The results presented here suggest how replacement of NH_3 with a planar amine may lead to significant changes in the rate of formation and structure of DNA adducts, differentiating these complexes from the "classical" DDP isomer. This work and ongoing studies on improved structural models will contribute to an understanding of the biological activity of nonclassical *trans* platinum antitumor complexes.

Acknowledgment. U.B. gratefully acknowledges support of a research fellowship from the Deutsche Forschungsgemeinschaft (DFG, Bonn, Germany). We thank Dr. Neel J. Scarsdale for setting up the NOESY experiment. U.B. wishes to thank Dr. Yun Qu and Dr. Marieke J. Bloemink for their help with processing NOESY data and for stimulating discussions. Thanks are also due to Johnson-Matthey, Ltd. (Reading, England), for a loan of K_2PtCl_4.

Supporting Information Available: Tables of AMBER force field parameters and fractional charges, plots of superimposed energy-minimized structures of **5** and **6**, an ^{1}H NMR stacked plot showing the progress of the reaction between **2** and 5′-GMP, a 2D COSY spectrum of **4** (aromatic and sugar proton regions), and a 1D ^{1}H NMR spectrum of **4** (sugar proton region) giving signal assignments (7 pages). Ordering information is given on any current masthead page.

IC970154O

(37) Bose, R. N.; Moghaddas, S.; Weaver, E. L.; Cox, E. H. *Inorg. Chem.* **1995**, *34*, 5878.

(38) Lambert, B.; Jestin, J.-L.; Bréhin, P.; Oleykowski, C.; Yeung, A. T.; Mailliet, P.; Prétot, C.; Le Pecq, J.-B.; Jacquemin-Sablon, A.; Chottard, J.-C. *J. Biol. Chem.* **1995**, *270*, 21251.

(39) Drlica, K.; Franco, R. J. *Biochemistry* **1988**, *27*, 2253.

(40) Osheroff, N. *Pharmacol. Ther.* **1989**, *41*, 223.

(41) Liu, L. F. In *DNA Topology and Its Biological Effects*; Wang, J. C., Cozzarelli, N. R., Eds.; CSH Laboratory Press: Cold Spring Harbor, NY, 1990; pp 371−389.

(42) Sundquist, W. I.; Bancroft, D. P.; Lippard, S. J. *J. Am. Chem. Soc.* **1990**, *112*, 1590.

(43) Neidle, S. In *DNA Structure and Recognition*; Rickwood, D., Ed.; IRL Press: Oxford, England, 1994; pp 71−96 and literature cited therein.